11 WCEE

Paper No. 177. (quote when citing this article)
Eleventh World Conference on Earthquake Engineering
ISBN: 0 08 042822 3

FAILURE MECHANISM UNDER REVERSED CYCLIC LOADING AFTER FLEXURAL YIELDING

H.KINUGASA and S.NOMURA

Department of Architecture, Science Univ. of Tokyo
Yamazaki, Noda city, Chiba, JAPAN

ABSTRACT

In this paper, a new failure mode peculiar to reversed cyclic loading is proposed. Under reversed cyclic loading, a shear–resisting mechanism repeats temporary disappearance and rebuilding because of the opening and closing of cracks. The proposed failure mode occurs when the shear–resisting mechanism can not be rebuilt after the temporary disappearance. This failure mode has been considered to be a kind of shear failure because of the rapid increase of shear deformation when it occurs. But the failure mechanism is different from that of shear failure. The proposed failure mode is not caused by increasing shear load, but is caused by a decrease in the stiffness of the cracked concrete.

KEYWORDS

Ductility; reversed cyclic loading; shear–resisting mechanism; lateral strain; confinement effect; reinforced concrete

INTRODUCTION

In order to establish a seismic design based on ultimate strength concepts, it is necessary to clarify cyclic behavior in large deformation range beyond flexural yielding. The purpose of this paper is to propose a new failure mode named "Reversed Cyclic Loading Failure", which occurs after flexural yielding. This failure mode has been considered to be a kind of "shear failure", because of the rapid increase of shear deformation when it occurs. In this paper, two kinds of specimen (Specimen A and B) were tested for comparison purposes of these failure modes. On the basis of the test results, the existence of the new failure mode and the difference of the failure mechanism were discussed.

SHEAR BENDING CYCLIC TESTS OF CANTILEVER R/C BEAM

Outline of Experiment

The details of the specimens A and B are shown in Fig.1. The strains were measured in the reinforcement shown in this figure. The test setup and the measuring arrangement are shown in Fig.2 and 3, respectively. From the measurement of the pinned loading point (see Fig.3 A.), the deflection angle R and the bending angle R_B, defined in Fig.4(a), were calculated. From the measurement of the plastic–hinging region (see Fig.3 B.C.), the lateral strain ε_L was calculated as shown in Fig.4(b). Most of the deformation was concentrated in the shadowed portion of Fig.4(b). Since the measured lateral strains on both sides of the plastic–hinging region (see Fig.3 C.) were very much similar before the occurrence of the strength deterioration, it was considered that the obtained lateral strains before the strength deterioration were reliable in spite of the damage.

Specimen A was tested under five different loading histories. These results are shown in Fig.6. In this paper, "Unloading", "Reloading" and "Reversed loading" are defined as shown in Fig.5. Specimens A−1,A−2 and A−3 were subjected to different reversed cyclic loading histories (see Fig.6(a),(b),(c)). On the other hand, specimen A−4 was subjected to monotonic loading (Fig.6(d)). And in case of specimen A−5, "Unloading" and "Reloading" were repeated toward one direction (Fig.6(e)). Specimen B was subjected to the same reversed cyclic loading as specimen A−1 (Fig.7). The material properties of the reinforcement are shown in table 1 and the concrete strength of each specimen is shown in Fig.6 and 7.

Strength Deterioration under Reversed Cyclic Loading

Specimen A−4 subjected to monotonic loading kept almost constant strength after flexural yielding, though the deflection angle R reached 200/1000 rad. (see Fig.6(d)). On the other hand, specimens A−1,A−2 and A−3 subjected to reversed cyclic loading failed between 40/1000 and 80/1000 rad. and rapid strength deterioration occurred (see Fig.6(a),(b),(c)). In the case of specimen A−5 subjected to unloading and reloading toward one direction, strength deterioration did not occur in spite of a lot of cyclic loading (see Fig.6(e)). These results suggest that the failure mechanism of specimens A−1,A−2 and A−3 is closely connected with reversed loading. The measured strains in these specimens indicated that yielding of the longitudinal bars occurred but yielding of the stirrups did not occur.

In case of specimen B, yielding of the stirrups was observed after flexural yielding and rapid strength deterioration occurred (see Fig.7). Since diagonal cracks formed and opened widely, it was considered that specimen B failed in shear failure obviously.

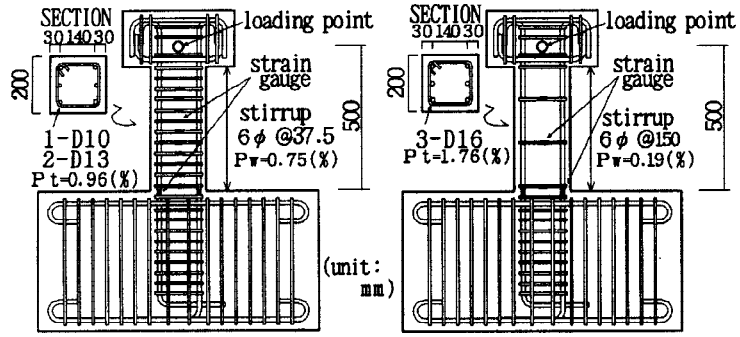

(a)Specimen A (b)Specimen B

Fig.1 Details of test specimen

Table 1 Material properties of reinforcement

		Yield Strength (kgf/cm²)	Tensile Strength (kgf/cm²)
Specimen A	6φ	4400	5000
	D10	4300	5900
	D13	4200	5800
Specimen B	6φ	3300	4300
	D16	4100	5700

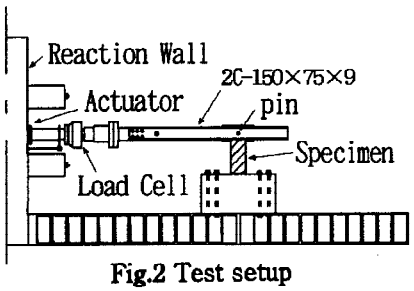

Fig.2 Test setup

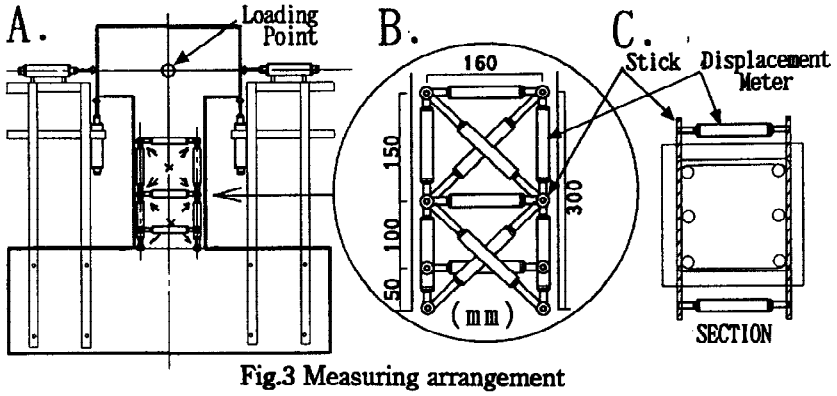

Fig.3 Measuring arrangement

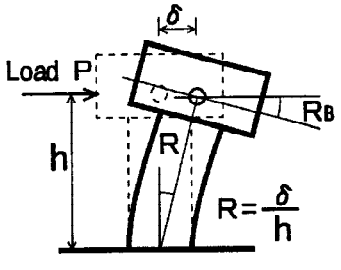

(a) Deflection Angle R and Bending Angle R_B

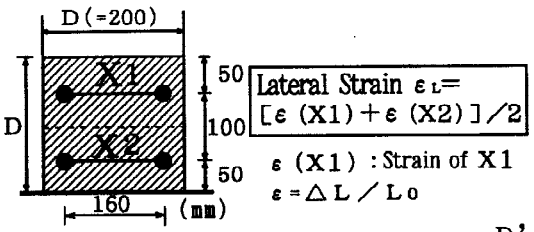

(b) Lateral Strain ε_L in plastic-hinging region

Fig.4 Deflection angle R, Bending angle R_B and Lateral strain ε_L

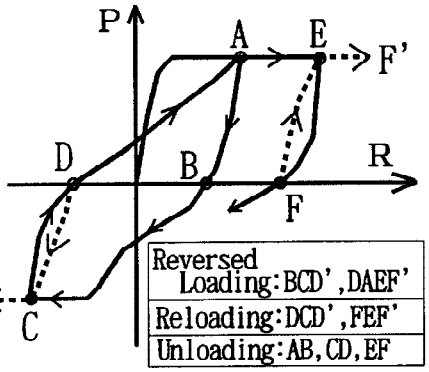

Fig.5 Loading

Temporary Disappearance and Rebuilding of Shear-resisting Mechanism

In order to clarify the behavior of the shear-resisting mechanism in the plastic-hinging region, the bending angle (R_B) - deflection angle (R) relationship was investigated. The decrease in the tangent slope shown in Fig.8 indicates an increase in the shear deformation ratio.

The R_B - R relationship of specimens A-4,A-5 and A-1 are shown in Fig.9. Under monotonic loading, the R_B - R relationship is approximately linear as shown in Fig.9(a). The linear behavior is also observed in specimen A-5 subjected to unloading and Reloading (see Fig.9(b)). On the other hand, in the case of specimen A-1 subjected to reversed loading, the R_B - R relationship does not show the linear behavior (see Fig.9(c)). The R_B - R relationship before the strength deterioration for specimen A-1 is shown in Fig.10(a). And Fig.10(b) is the corresponding load P - deflection angle R relationship. In addition to the same linear behavior as monotonic loading

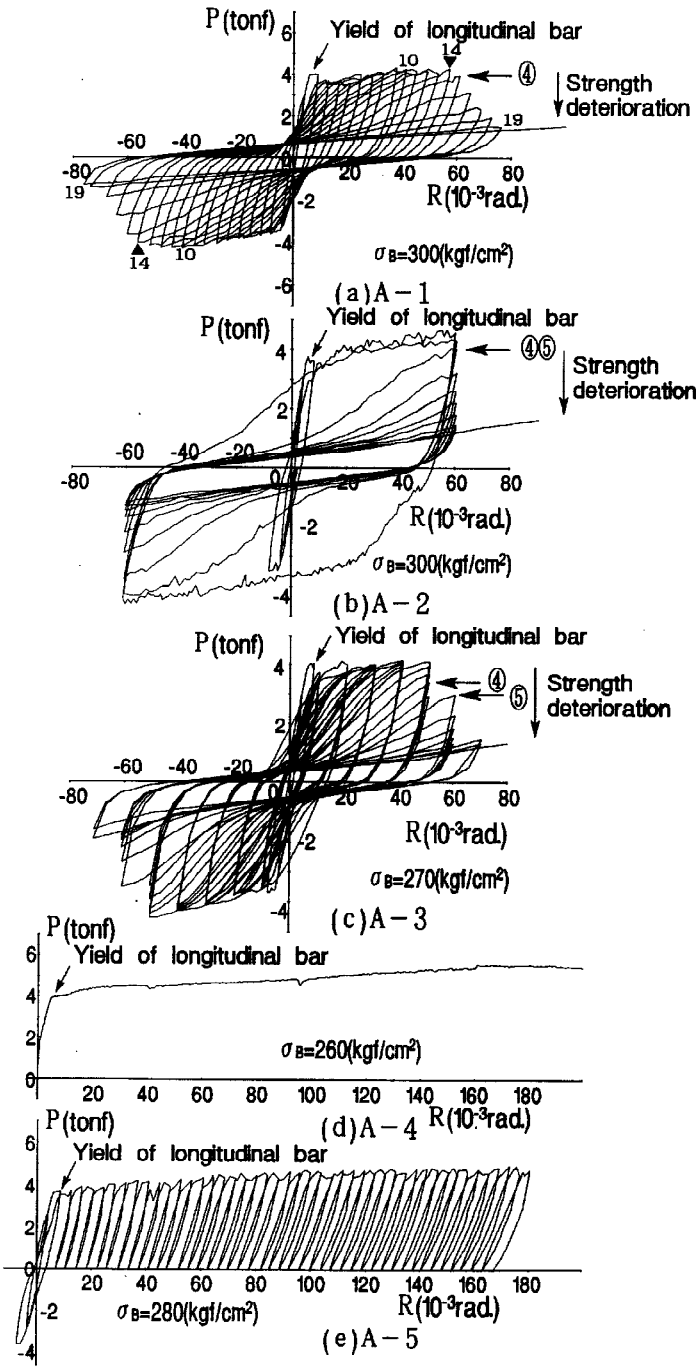

Fig.6 Load P- Deflection angle R relationship (Specimen A)

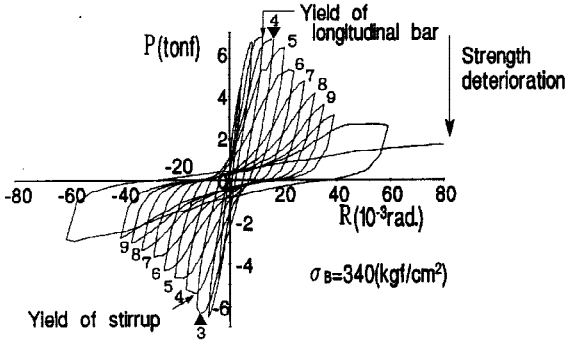

Fig.7 Load P- Deflection angle R relationship (Specimen B)

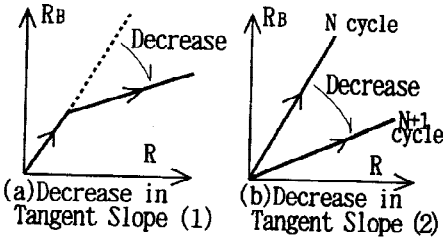

Fig.8 Increase behavior of shear deformation

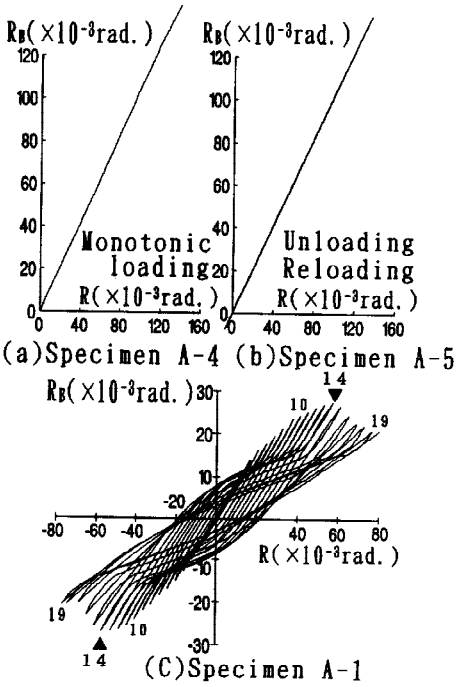

Fig.9 Bending angle R_B -Deflection angle R relationship

(③④ and ⑥① in Fig.10(a)), non linear behavior(②③ and ⑤⑥ in Fig.10(a)) is observed. Since the non linear behavior occurs at the beginning of reversed loading where the specimen stiffness decreases (see ②③ and ⑤⑥ in Fig.10(b)) and the tangent slope recovers as shear load increases (②③④ and ⑤⑥① in Fig.10(a)), the non linear behavior (deterioration of shear stiffness) is considered to be caused by temporary disappearance of the shear−resisting mechanism due to the opening and closing of cracks under reversed loading. Fig.10(a) indicates that the shear−resisting mechanism repeats temporary disappearance (②③ and ⑤⑥ in Fig.10(a)) and rebuilding (③④ and ⑥① in Fig.10(a)) because of the disappearance of the concrete strut under reversed loading (see ①②③ in Fig.11). The temporary disappearance (②③ and ⑤⑥ in Fig.10(a)) does not occur without reversed loading as shown in Fig.9(a),(b).

New Failure Mode under Reversed Cyclic Loading

The $R_B - R$ relationship for specimen B which failed in shear failure is shown in Fig.13(a). And Fig.13(b) shows the $R_B - R$ relationship after the strength deterioration. The corresponding P−R relationship is shown in Fig.13(c).

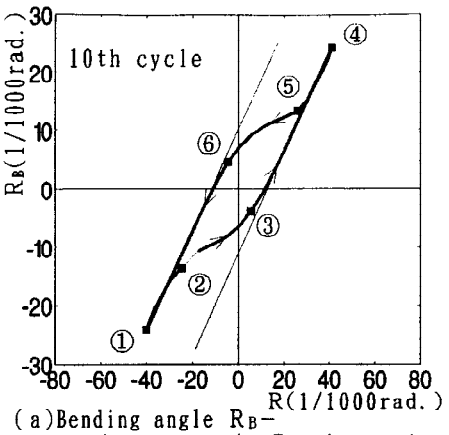

(a)Bending angle R_B− Deflection angle R relationship

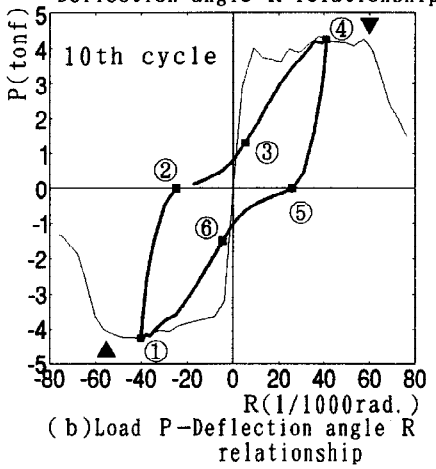

(b)Load P−Deflection angle R relationship

Fig.10 R_B −R and corresponding P−R relationship before strength deterioration(Specimen A−1)

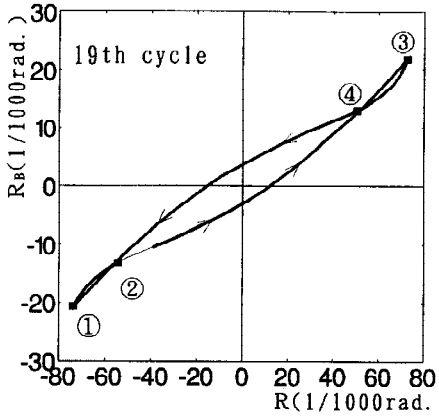

(a)Bending angle R_B− Deflection angle R relationship

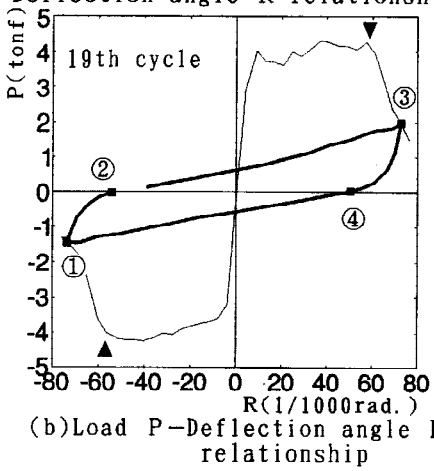

(b)Load P−Deflection angle R relationship

Fig.12 R_B −R and corresponding P−R relationship after strength deterioration(Specimen A−1)

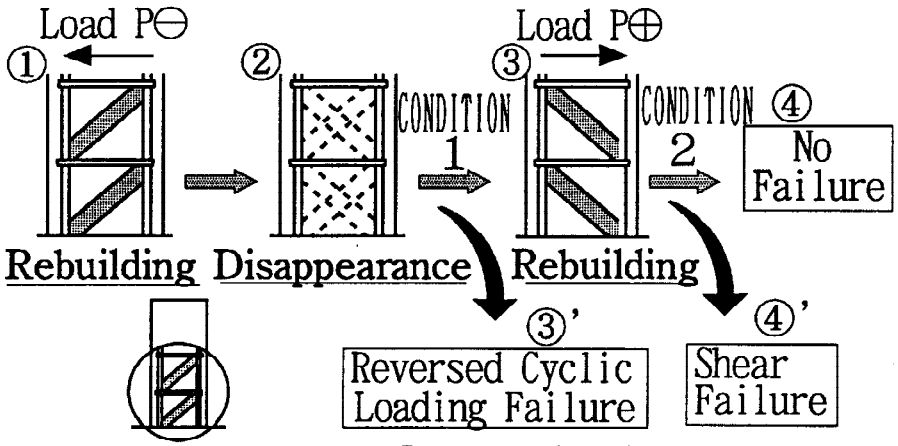

Fig.11 Failure mechanism of Reversed cyclic loading failure

Under reversed loading (②③④⑤ and ⑥⑦⑧① in Fig.13(c)), a decrease in the tangent slope at the beginning of reversed loading (②③ and ⑥⑦ in Fig.13(b)) and a decrease in the tangent slope just before peak load (④⑤ and ⑧① in Fig.13(b)) are observed. The first decrease in the tangent slope (②③ and ⑥⑦ in Fig.13(b)) is considered to be caused by the temporary disappearance of the shear−resisting mechanism described above, since the tangent slope recovers as shear load increases (③④ and ⑦⑧ in Fig.13(b)). And the second decrease (④⑤ and ⑧① in Fig.13(b)) is considered to be caused by the destruction of the rebuilt shear−resisting mechanism due to increasing shear load. In the case of specimen B, the shear failure process (① rebuilding →② disappearance → ③ rebuilding →④ 'destruction) shown in Fig.11 is confirmed from the deformation behavior. The $R_B - R$ curves just before peak load (⑦⑧① in Fig.13(b)) are picked up and shown in Fig.14(a). From the cycle where the strength deterioration occurs (from ▼ in Fig.14(a)), the decrease in the tangent slope shown in Fig.8(a) is observed remarkably. The decrease behavior shown in Fig.8(a) should be observed when the destruction of the shear−resisting mechanism due to increasing shear load occurs.

The $R_B - R$ relationship after the strength deterioration for specimen A−1 is shown in Fig.12(a). And the corresponding P−R relationship is shown in Fig.12(b). As seen in this figure, the decrease behavior shown in Fig.8(a) does not appear (see ②③ and ④① in Fig.12(a)). The $R_B - R$ curves just before peak load (③④ in

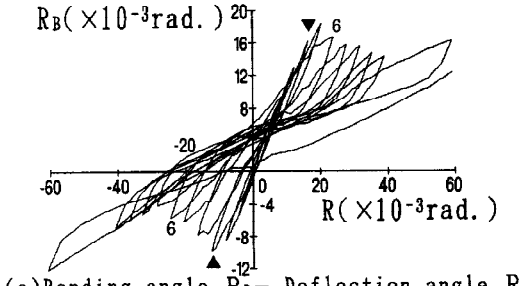

(a)Bending angle R_B− Deflection angle R relationship

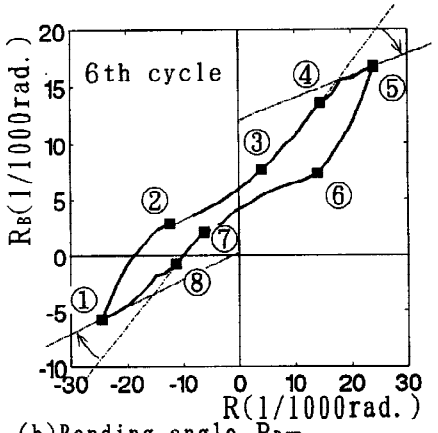

(b)Bending angle R_B− Deflection angle R relationship

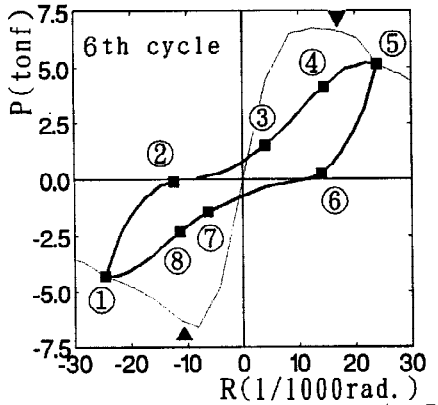

(c)Load P−Deflection angle R relationship

Fig.13 R_B −R and corresponding P−R relationship after strength deterioration (Specimen B)

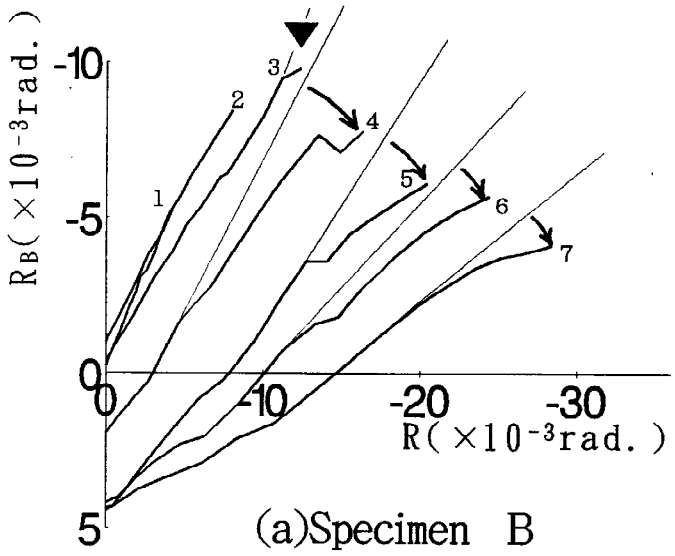

(a)Specimen B

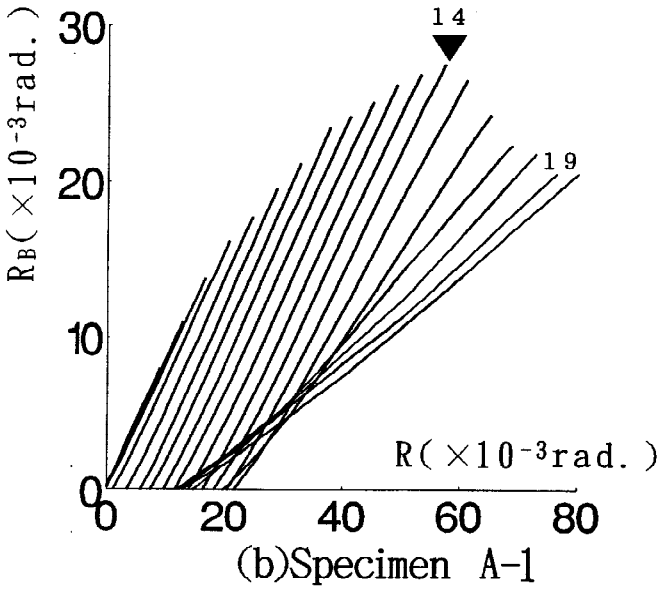

(b)Specimen A-1

Fig.14 Increase behavior of shear deformation

Fig.10(a)) are picked up and shown in Fig.14(b). From the cycle where the strength deterioration occurs (from ▼ in Fig.14(b)), the decrease behavior shown in Fig.8(b) is observed. But the decrease behavior shown in Fig.8(a), which indicates the occurrence of the destruction of the shear-resisting mechanism due to increasing shear load, does not appear. Comparing Fig.14(b) with Fig.14(a), the difference of the failure behavior between specimen A and B is obvious. It is considered that the strength deterioration of specimen A is not caused by the destruction of shear-resisting mechanism due to increasing shear load.

Before the strength deterioration (before ▼ in Fig.14(b)), the $R_B - R$ relationship for specimen A shows linear behavior and has almost the same tangent slope. These results indicate that the shear-resisting mechanisms rebuilt before the strength deterioration have almost the same characteristics, and that the strength deterioration of specimen A occurs when the shear-resisting mechanism which has been maintained can not be rebuilt after the temporary disappearance (see ①②③' in Fig.11). The quality of the rebuilding is considered to be affected by the stiffness deterioration of the cracked concrete in the plastic-hinging region.

LATERAL STRAIN IN THE PLASTIC-HINGING REGION

Lateral Strain ε_L and Strength Deterioration

The lateral strain ε_L of the plastic-hinging region versus dissipated energy relationship is shown in Fig.15. In the specimens A-1,A-2,A-3 and B, strength deterioration was observed. The lateral strain of specimen B increases rapidly because of the yielding of the stirrups. On the other hand, the lateral strain of specimen A also increases in spite of no yielding of the stirrups. Marks ④ and ⑤ in Fig.6 show the cycle where the lateral strain of specimen A reaches 4 % and 5 % respectively. These cycles agree with the beginning of the strength deterioration (see Fig.6(a)(b)(c)). In the same manner as specimen B, the increase in the lateral strain of specimen A is closely connected with the strength deterioration. These results observed in specimen A suggest that the stiffness deterioration of the core concrete caused by the lateral strain obstructs the rebuilding of the shear-resisting mechanism after the temporary disappearance.

The increase in the lateral strain observed in specimen B is considered to be caused by the axial deformation of the stirrups shown in Fig.16(a). In the case of the lateral strain observed in specimen A, the deflection of the stirrups shown in Fig.16(b) was visually observed at the end of the test.

Increase Behavior of Lateral Strain ε_L

The lateral strain ε_L - deflection angle R relationship for specimen B is shown in Fig.17(a). And the corresponding P-R relationship is shown in Fig.17(b). Under reversed loading (④⑤⑥ in this figure), the lateral strain increases and the rate of increase ($d\varepsilon_L/dR$) continues to rise (see ④⑤⑥ in Fig.17(a)). As described above, yielding of the stirrups was observed in specimen B. Considering the stiffness deterioration of the stirrups due to the yielding, the increase in the rate ($d\varepsilon_L/dR$) should be observed as the deflection angle R increases.

The $\varepsilon_L - R$ relationship for specimen A-1 is shown in Fig.18(a). And the corresponding P-R relationship is shown in Fig.18(b). Under the reversed loading ①② where the shear-resisting mechanism temporarily disappears, the

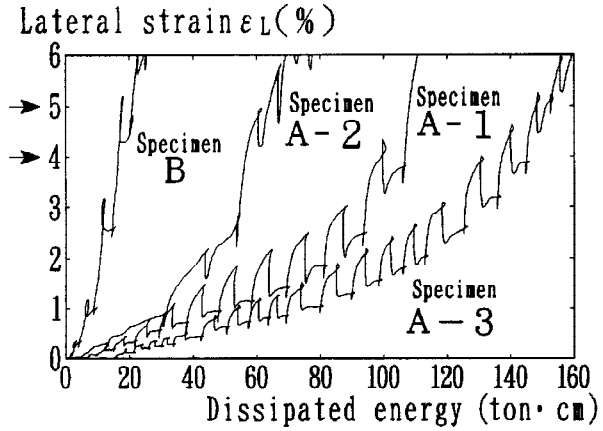

Fig.15 Increase in lateral strain ε_L

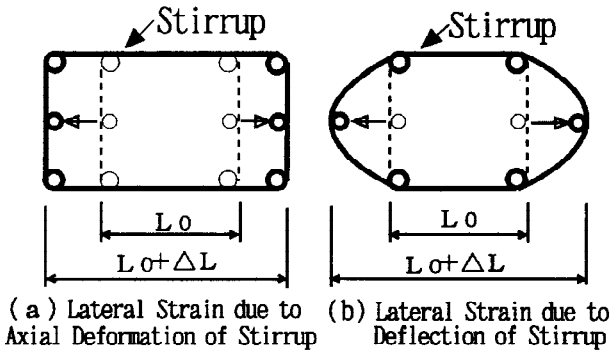

Fig.16 Lateral strain ε_L and deformation of stirrup

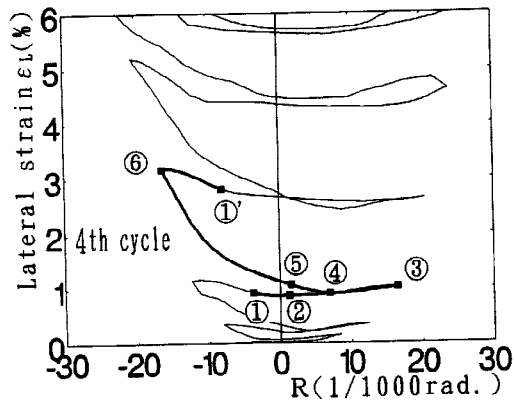

(a)Lateral strain ε_L – Deflection angle R relationship

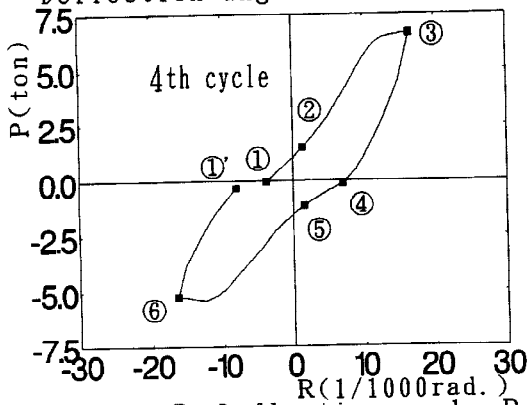

(b)Load P – Deflection angle R relationship

Fig.17 Increase behavior of lateral strain ε_L (Specimen B)

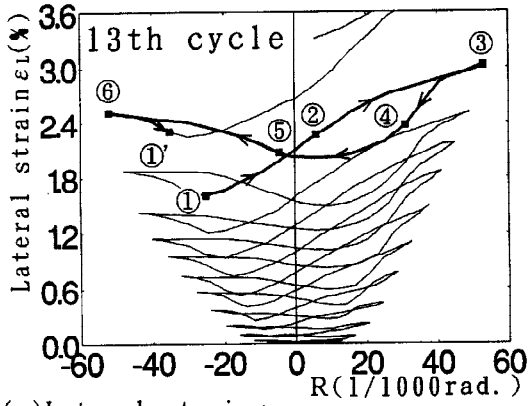

(a)Lateral strain ε_L – Deflection angle R relationship

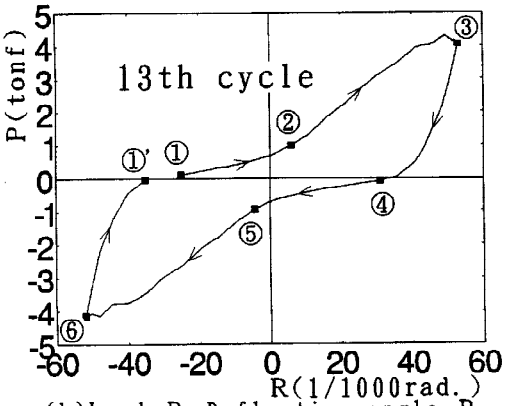

(b)Load P – Deflection angle R relationship

Fig.18 Increase behavior of lateral strain ε_L (Specimen A–1)

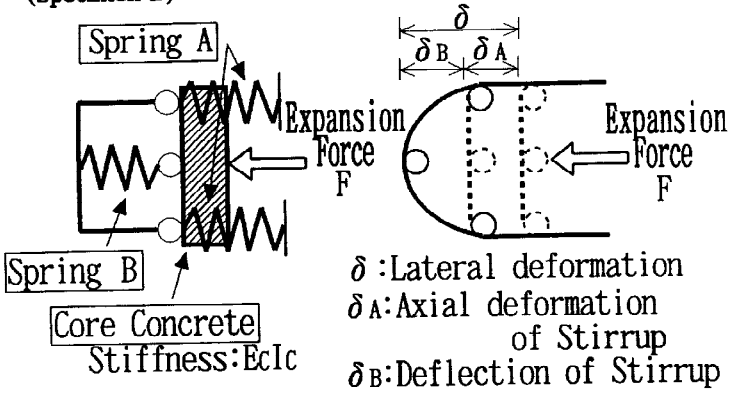

Fig.19 Analytical model of confinement

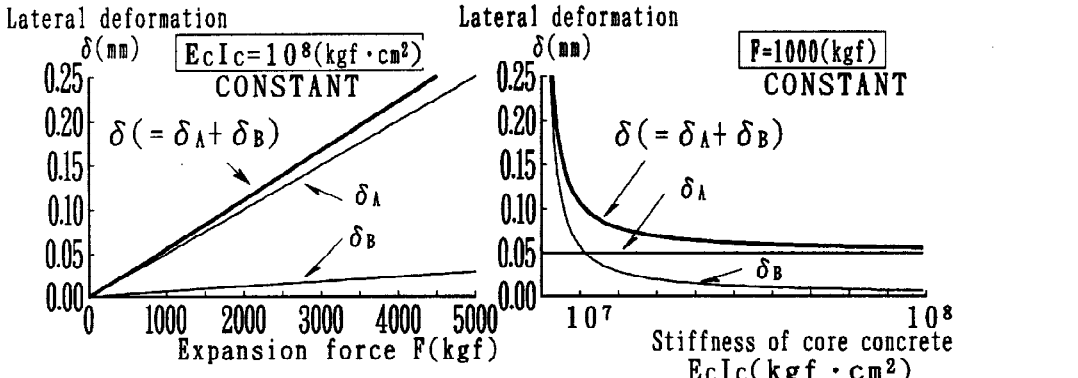

(a)Lateral deformation due to expansion force

(b)Lateral deformation due to a decrease in stiffness of core concrete

Fig.20 Results of analysis

lateral strain increases and the rate of increase ($d\varepsilon_L/dR$) rises in the same manner as specimen B (see ①② in Fig.18(a)). On the other hand, under the loading ②③ where the shear-resisting mechanism is rebuilt, the lateral strain increases but the rate of increase ($d\varepsilon_L/dR$) gradually decreases (see ②③ in Fig.18(a)) . When the shear-resisting mechanism disappears (①② in Fig.18(a)), the stiffness of the core concrete is considered to decrease because of the disappearance of the concrete strut (see ② in Fig.11). The increase mechanism of the lateral strain observed in specimen A is considered to be different from that of shear failure and is closely connected with the stiffness deterioration of the core concrete.

Increase Mechanism of Lateral Strain

The purpose of this analysis is to investigate the increase mechanism of the lateral strain observed in specimen A, qualitatively. The analytical model is shown in Fig.19. A simply supported beam is used to represent the core concrete, and expansion force (F) provided by shear load is placed at the midspan as shown in Fig.19. In order to model the confinement by stirrups, two kinds of spring are used. One (spring A) represents the axial deformation of stirrups (δ_A) shown in Fig.16(a) and the other (spring B) represents the deflection of stirrups (δ_B) shown in Fig.16(b). The stiffness of the spring A is assumed to be 100 times as large as the stiffness of the spring B.

Calculations are carried out under the following two analytical conditions: Analytical condition 1. The expansion force (F) increases under the condition that the stiffness of the core concrete ($E_c I_c$) is kept constant. Analytical condition 2. The stiffness of the core concrete ($E_c I_c$) decreases under the condition that the expansion force (F) is kept constant. Fig.20(a) shows the result obtained under the analytical condition 1. The lateral deformation (δ) increases as the expansion force (F) increases. The lateral deformation (δ) is mainly caused by the axial deformation of the stirrups (δ_A) (see Fig.16(a)). It is considered that the increase in the lateral strain observed in specimen B which failed in shear failure is caused by the deterioration of confinement due to the expansion force (F) provided by shear load. On the other hand, Fig.20(b) shows the result obtained under the analytical condition 2. The lateral deformation (δ) increases as the stiffness of the core concrete ($E_c I_c$) decreases, though the expansion force (F) is kept constant. The axial deformation of the stirrups (δ_A) (see Fig.16(a)) is kept constant but the deflection deformation (δ_B) (see Fig.16(b)) increases. The analytical results suggest that the core concrete passes between the corner longitudinal bars as the stiffness of the core concrete decreases. It is considered that the increase of the lateral strain observed in specimen A is caused by the deterioration of confinement due to the decrease in the stiffness of the core concrete.

CONCLUSION

The strength deterioration of specimen A is caused by "Reversed cyclic loading failure". Under reversed cyclic loading, a shear-resisting mechanism in the plastic-hinging region repeats temporary disappearance and rebuilding because of the opening and closing of cracks (see ①②③ in Fig.11). Before the strength deterioration, the shear-resisting mechanisms, which are rebuilt after the temporary disappearance, have almost the same characteristics. In order to maintain the strength under reversed cyclic loading, it is necessary to satisfy the following two conditions : Condition 1. The shear-resisting mechanism which has temporarily disappeared is rebuilt (②③ in Fig.11). Condition 2. The rebuilt shear-resisting mechanism is not destroyed by shear load (③④ in Fig.11). Shear failure occurs when the condition 2 is not satisfied (see ③④ ' in Fig.11). On the other hand, "Reversed cyclic loading failure" occurs when the condition 1 is not satisfied (see ②③ ' in Fig.11). "Reversed cyclic loading failure" does not occur without the temporary disappearance of shear-resisting mechanism, which is caused by the opening and closing of cracks under reversed loading. This indicates that the proposed failure mode is peculiar to reversed cyclic loading.

It is considered that an increase in the lateral strain of the plastic-hinging region obstructs the rebuilding of the shear-resisting mechanism. There are two kinds of deterioration mechanism of confinement. Ⓐ . Deterioration by increasing the expansion force which is provided by shear load (see Fig.20(a)). Ⓑ . Deterioration by decreasing the stiffness of the core concrete (see Fig.20(b)). In case of "Reversed cyclic loading failure", the lateral strain is caused by the second deterioration mechanism of confinement. When the shear-resisting mechanism temporarily disappears because of reversed loading, the stiffness of the core concrete decreases because of the disappearance of the concrete strut (see ② in Fig.11). That causes the increase of the lateral strain because of the second deterioration mechanism of confinement. And the increase in the lateral strain causes more stiffness deterioration of the core concrete, and this causes more increase in the lateral strain because of the second deterioration mechanism again. "Reversed cyclic loading failure" occurs when the stiffness of the core concrete becomes too small to rebuild the shear-resisting mechanism after the temporary disappearance. The proposed failure mode is not caused by increasing shear load but caused by reversed loading and the stiffness deterioration of cracked concrete due to that.